2005 American Control Conference
June 8-10, 2005. Portland, OR, USA

Modeling and Control of Two Stage Twin Spool Servo-Valve for Energy-Saving

QingHui Yuan and Jae Y. Lew

Abstract— **A control strategy of two stage twin spool servovalves in the load-sensing mobile applications is presented. The twin spool valve differs from the conventional valve in that it provides the ability to control flow into and out of valves independently. In this paper, the nonlinear valve model and a control scheme for a two stage twin spool servo-valve are developed featuring energy saving. The multiple sliding surface mode control method is then utilized to accomplish the motion control while regulating back pressure. The simulation verifies that the proposed control scheme for the twin spool valve, can offer the more significant energy-saving even with load-sensing pump application than the traditional proportional valves.**

I. Introduction

The fluid power industry is conventionally classified into industrial and mobile hydraulics. In industrial hydraulics, the power supply can be set to be sufficient to satisfy the system requirement regarding both flow and pressure [1]. However, when it comes to mobile hydraulics, it becomes challenging. The demanding requirements, like the changing environment, limited space, and higher power/weight ratio, necessitate the reliability and adaptiveness of the hydraulic components and system. In particular, considering the fact that the primary power source is a single diesel engine on each machine, energy efficiency of the hydraulic system becomes a very important issue. Higher energy efficiency is preferred to avoid the excess of limited diesel power. Moreover, the better temperature balance can be achieved since less power losses implies less heat. Then the smaller oil cooler can be used in the system, and the overall cost of the machine can be lowered down.

In current mobile applications, load-sensing pumps are considered among the most promising solutions for energy-saving. Compared with constant displacement pumps and even variable displacement pumps with constant pressure compensation, the load-sensing pumps can provide us with the tremendous energy-saving. The detailed comparison of energy consumption for the above three types of pumps can be found in some recent investigations [1] [2]. For a load-sensing pump used in a single-acting hydraulic actuator, the minimum wasted energy can be the multiplication of the marginal pressure P_m by the supply flow rate Q_s [2]. In this paper, we address the energy-saving issue in double-acting hydraulic actuators with a two-stage twin-spool servovalve.

Energy-saving feature of load-sensing system is directly associated with the mobile proportional valve. For a typical proportional valve, a single main spool is stoked via direct-acting solenoids or hydraulic pilot-operation. When the spool moves, the meter-in and meter-out orifice areas can change simultaneously to control the flow rate into and out of the chambers of a hydraulic cylinder. Since the longer single spool causes the stringent manufacturing tolerances and the complicated assembly precess, an alternative design, a two stage twin spool flow control servovalve [3] [4] , has been provided. Two separate main spools that independently meter flow into and out of the valve, reduce the cost for manufacturing and assembly, and enhance the reliability of the system, thus being very suitable for mobile hydraulics. The twin spools move identically via hydraulic pilot operation as they were virtually connected. For such a design, however, it is reasonable to ask: Why the twin spools should be virtually connected, or move independently? Is it possible to gain the extra benefit of energy-saving if the twin spools are controlled independently?

Fig. 1. Cutaway of a two stage twin spool valve (courtesy of Eaton Corporation).

In this paper, we present the concept of controlling a two stage twin spool servovalve. The difference that separates our work from the previous research [3] [4] is that we modify the pilot stage in such a way that the twin spool displacements can be controlled independently. A cutaway view of the two stage twin spool valve is illustrated in Fig. 1. In addition, we propose to achieve the multiple control objectives, both the flow control and the pressure control, based on multiple sliding surface control law. The controller can offer the benefit of energy-saving compared with the traditional proportional valve.

The rest of the paper is organized as follows. In section II, the mathematic model of such a two stage twin spool valve is developed. Section III presents the sliding mode controller to regulate the back pressure and control the motion of a hydraulic actuator. In Section IV, simulation results based on a backhoe loader are discussed. The energy-saving feature of such a valve is addressed in Section V. The concluding remarks are given in Section VI.

QingHui Yuan is with the Department of Mechanical Engineering, University of Minnesota, Minneapolis, MN 55455. qhyuan@me.umn.edu.
Jae Y. Lew is with Eaton Corporation Innovation Center, Eden Prairie, MN. JaeYLew@eaton.com.

II. VALVE DYNAMICS

A schematic of the two stage twin spool flow control valve is shown in Fig. 2. The pilot stage consists of two independent four-land four-way spool valves. Each spool is actuated by a voice coil linear motor to control the pressures in the end chambers of the boost stage. The main stage consists of two independent two-land three-way spool valves. These spools are spring centered, and actuated via pressure at the end chambers. For simplicity, the following section only contains the dynamics of the left half part of the system in Fig. 2. The similar dynamics of the right half part is not included. Later, it is shown that the dynamics of two spools are coupled through the double acting actuator.

A. Voice coil motor dynamics

For the left side spool in the pilot stage, a voice coil actuator (which is not shown in Fig. 2) is used to stroke the spool. In general, a voice coil actuator can be modeled in a similar way to a DC motor. It produces a force that is proportional to the current driven through the actuator

$$F_{vc1} = K_{vc} i_1 \tag{1}$$

where K_{vc} is the force constant with units of N/A, i_1 is the current though the actuator. If we apply the voltage u_1 across the coil, the dynamics of the electric circuit is governed by

$$L\frac{d}{dt}i_1 + Ri_1 + K_{vc}\dot{x}_1 = u_1 \tag{2}$$

where L, R are the inductance and the resistance of the voice coil actuator, x_1 is the spool displacement, and K_{vc} is related to the back electromotive.

B. Pilot stage spool dynamics

We assume that the transient flow forces applied on the pilot spool are negligibly small. From Newton's Second Law, we have the spool dynamics as follows

$$M\frac{d}{dt}\dot{x}_1 = F_{vc1} + F_{fp} + K_{vp}\dot{x}_1 \tag{3}$$

in which M is the pilot spool mass, F_{vc1} is the force produced by the voice coil motor in Eq. (1), and F_{fp} is the flow induced force [5], and K_{vp} is the viscous damping coefficient.

C. Main stage dynamics

Similarly, the main stage spool dynamics can be obtained

$$M_m\frac{d}{dt}\dot{x}_{v1} = -K_s x_{v1} - K_v\dot{x}_{v1} + (P_{11} - P_{12})A + F_{fm} \tag{4}$$

where M_m is the spool mass in the second stage, x_{v1} is the displacement of the spool, K_s is the spring coefficient that is determined by the type of the spring, K_v is the viscous damping coefficient that is obtained from [5], A is the cap area of the spool contacting the end chambers, P_{11}, P_{12} are the chamber pressures, and F_{fm} is the flow induced forces.

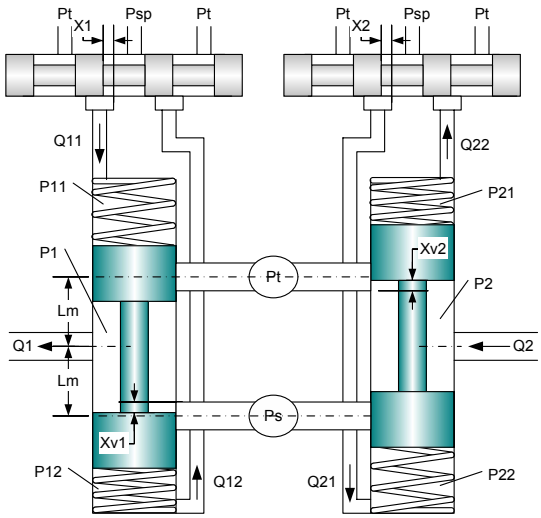

Fig. 2. Diagram of two stage twin spool valve. The pressures P_1, P_2 and the displacements x_{v1}, x_{v2} are measured via sensors.

D. Chamber pressure dynamics

The chamber pressure dynamics are determined by compressibility of the fluid in the chambers between the pilot stage and the main stage.

$$\frac{d}{dt}P_{11} = \frac{\beta_e}{V_{11}}\left(Q_{11} - A\dot{x}_{v1}\right) \tag{5}$$

$$\frac{d}{dt}P_{12} = \frac{\beta_e}{V_{12}}(A\dot{x}_{v1} - Q_{12}) \tag{6}$$

in which P_{11}, P_{12} are the pressures in the upper and lower chamber, respectively, Q_{11}, Q_{12} are the flow rate into the upper chamber and out of the lower chamber, β_e is the bulk modulus of hydraulic fluid, V_{11}, V_{12} are the volumes in the upper and lower chambers.

III. MOTION AND PRESSURE CONTROLLER DESIGN

A. Controller configuration

The diagram of a typical hydraulic control system utilizing a twin spool valve is shown in Fig. 3, in which the controllers are configured in a cascade manner. In other words, we have an inner-loop controller $C(s)$ and a outer-loop controller D. Based on the valve models, an inner-loop controller $C(s)$ is designed so that the twin spool displacements x_{v1}, x_{v2} track the command x_{v1d}, x_{v2d}. Note that the valve dynamics are linearized at an equilibrium point. The linear models can be verified via the comparison of the step responses from the voice coil motor voltages u_1, u_2 to the main stage spool displacements x_{v1}, x_{v2} for the nonlinear and linear models as suggested in [4]. Using the linear control theory, a linear controller $C(s)$ can be so chosen that the transient response is as fast as possible. The details of the design can be referred to [5] [6].

The outer-loop controller D design is presented as follows.

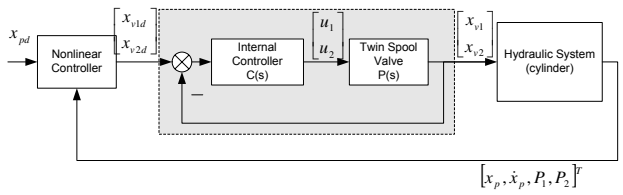

Fig. 3. Block diagram of the twin spool valve hydraulic control system.

B. Outer-loop controller D

In Fig. 3, we assume the inner-loop dynamics are very fast so that we can neglect them while designing D. The controller is designed with two objectives: position tracking and energy saving.

We will consider a single-rod double-acting hydraulic actuator with unidirectional external load, as shown in Fig. 4. If we neglect the internal & external leakages and the internal dynamics of valve, the dynamics of the hydraulic actuator can be modeled as

$$\begin{aligned}\ddot{x}_p &= \frac{1}{M_p}(P_1A_1 - P_2A_2) + \frac{1}{M_p}F_l \\ \dot{P}_1 &= \frac{\beta_e}{V_1(x_p)}(-A_1\dot{x}_p + Q_1) \\ \dot{P}_2 &= \frac{\beta_e}{V_2(x_p)}(A_2\dot{x}_p - Q_2)\end{aligned} \tag{7}$$

where x_p, M_p is the displacement and the mass of the rod, A_1, A_2, as illustrated in Fig. 4, are the cross area of the two chambers, P_1, P_2 are the pressures inside the two chambers of the cylinder, which are identical to the pressures between two lands of the main spool in Fig. 2 respectively, $V_1(x_p), V_2(x_p)$ are the chamber volumes of the actuator, and the flow rates into the chamber 1 and out of the chamber 2 are defined to be

$$Q_1(x_{v1}, P_1, P_s) = \begin{cases} C_dWx_{v1}\sqrt{2(P_s - P_1)/\rho}, & x_{v1} \geq 0; \\ C_dWx_{v1}\sqrt{2(P_1 - P_t)/\rho}, & x_{v1} < 0. \end{cases} \tag{8}$$

$$Q_2(x_{v2}, P_2, P_s) = \begin{cases} C_dWx_{v2}\sqrt{2(P_2 - P_t)/\rho}, & x_{v2} \geq 0; \\ C_dWx_{v2}\sqrt{2(P_s - P_2)/\rho}, & x_{v2} < 0. \end{cases} \tag{9}$$

As shown in the hydraulic circuit in Fig. 4, the load force F_l applied on the piston is unidirectional (leftward). This assumption is valid in some mobile applications. For instance, as the hydraulic actuator is used to provide the booming motion of a backhoe, the unidirectional force on the piston is produced by the heavy weight of the boom, the dipper, the bucket, and the variable loads.

The back pressure is then defined to be one in the chamber opposite to the external load direction (P_2). If $\dot{x}_p > 0$, the work port connection is $P_1 - P$ and $P_2 - T$, then there will be more energy wasted for nothing if the back pressure P_2 is large. If $\dot{x}_p < 0$, we have two possible choices of work port connection: (1) $P_1 - P$ and $P_2 - P$; (2)$P_2 - P$ and $P_1 - T$. Choice (1) is also called flow regeneration connection, where the flow is directly fed from

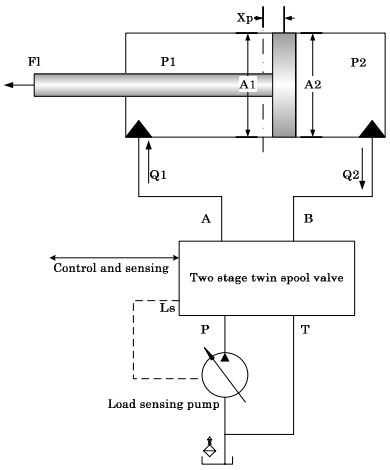

Fig. 4. Motion control of single-rod hydraulic actuator using two stage twin spool servovalve. The unidirectional load is assumed in this scenario. The load sensing port of the valve L_s, which is not illustrated in Fig. 2, connects with the pressure compensation port of the load sensing port, so that the load sensing pump provides the system with the desired pressure.

P_1 to P_2, and the pump is used to provide the flow into the chamber P_2 due to the differential area of the piston. There may be cavitation issue associated with Choice (1). For Choice (2), note that the external load injects the energy into the hydraulic system, which eventually dissipated in the passage $P_1 - T$. Likewise, lowering P_2 would help to reduce the energy loss at $P_1 - T$. In addition, we only need lower supply pressure P_s, otherwise there will be larger pressure drop across P_s and P_2. More detailed discussion can be found in Sec V. In short, regulating the back pressure P_2 help reduce the energy loss.

1) Back pressure regulation control:

As aforementioned, the objective is to regulate the pressure P_2 to a low desired value P_0 by controlling Q_2, or x_{v2}. From Eq. (7), we can set $Q_2 = Q_{2d}$ as a linear controller plus a feedforward term, where the desired flow rate is

$$Q_{2d} = A_2\dot{x}_p + \frac{V_2}{\beta_e}\lambda_2(P_2 - P_0) \tag{10}$$

for $\lambda_2 > 0$, so that the dynamics of P_2 is given to be $\dot{P}_2 = -\lambda_2(P_2 - P_0)$, i.e., P_2 converges to P_0 exponentially. From Eq. (8), we can define the desired spool displacement x_{v2d} as a function of Q_{2d}

$$x_{v2d}(Q_{2d}, P_s, P_2) = \begin{cases} \frac{Q_{2d}}{C_dW}\sqrt{\frac{\rho}{2(P_2 - P_t)}}, & Q_{2d} \geq 0; \\ \frac{Q_{2d}}{C_dW}\sqrt{\frac{\rho}{2(P_s - P_2)}}, & Q_{2d} < 0. \end{cases} \tag{11}$$

Therefore, the control input is $u_2 = C(s)(x_{v2d} - x_{v2})$, where $C(s)$ is the internal controller for the valve.

2) Piston position tracking:

To determine the required control effort, a multiple sliding surface control law [7] is designed to achieve tracking of the desired position trajectory. First we define the pressure force sliding manifold as follows:

$$s_1(F_p) = \dot{e}_p + \lambda_1 e_p = 0 \tag{12}$$

where the position error $e_p = x_p - x_{pd}$, the velocity error $\dot{e}_p = \dot{x}_p - \dot{x}_{pd}$, $\lambda_1 > 0$ is the desired pole, and the pressure force

$$F_p(P_1, P_2) = P_1 A_1 - P_2 A_2 \tag{13}$$

On this manifold, the motion is governed by $\dot{e}_p + \lambda_1 e_p = 0$, i.e., it can be guaranteed that $e_p \to 0$ exponentially. Taking the derivative of Eq. (12) gives

$$\begin{aligned} \dot{s}_1(F_p) &= \ddot{x}_p - \ddot{x}_{pd} + \lambda_1(\dot{x}_p - \dot{x}_{pd}) \\ &= \frac{1}{M_p}(\underbrace{P_1 A_1 - P_2 A_2}_{F_p} + F_l) - \ddot{x}_{pd} + \lambda_1(\dot{x}_p - \dot{x}_{pd}) \end{aligned} \tag{14}$$

Obviously, we apply the pressure force $F_p = F_{pd}$, in which the desired pressure force is

$$F_{pd} = M_p[\ddot{x}_{pd} - \lambda_1(\dot{x}_p - \dot{x}_{pd})] - \bar{F}_l \cdot sgn(s_1) \tag{15}$$

where $\bar{F}_l$ is a constant representing the upper bound of unknown load force. Then we have

$$\dot{s}_1 = (-\bar{F}_l \cdot sgn(s_1) + F_l)/M_p \tag{16}$$

where $\bar{F}_l$ is chosen to be sufficiently large so that $\exists \epsilon > 0$, the inequality $\bar{F}_l > |F_l(t)| + \epsilon M_p$ holds.

With $V = \frac{1}{2}s_1^2$ as a Lyapunov function candidate, Eq. (16) yields

$$\dot{V} = s_1 \dot{s}_1 \leq -\epsilon |s_1| \tag{17}$$

It is clear that the trajectory reaches the manifold $s_1 = 0$ in finite time [8], if we choose P_1, P_2 so that $F_p(P_1, P_2) = F_{pd}$.

Unfortunately, the actual control is $[Q_1, Q_2]^T$, or $[x_{v1}, x_{v2}]^T$. The pressure dynamics are governed by Eq. (7), so P_1, P_2 cannot be controlled directly. However, if P_1, P_2 can be controlled in such a way, using Q_1, Q_2, so that $F_p - F_{pd} = 0$, then $s_1(F_p)$ would converge to 0. A second sliding manifold, $s_2(Q_1, Q_2)$ is introduced as follows

$$s_2(Q_1, Q_2) = F_p - F_{pd} \tag{18}$$

It is clear that the controls can be determined by taking derivative of Eq. (18) once. In order to avoid the problem due to the discontinuous function $sgn(\cdot)$ in Eq. (15), an uniformly bounded C^∞ function $\widehat{sgn}(s_1)$ is used to approximate $sgn(s_1)$

$$\widehat{sgn}(s_1) = \frac{2}{\pi}\arctan(\alpha s_1) \tag{19}$$

where $\alpha \in R^+$ is sufficiently large so that the error $sgn(s_1) - \widehat{sgn}(s_1)$ is very small. Therefore, we have

$$\begin{aligned} \dot{F}_{pd} &\approx M_p[\dddot{x}_{pd} - \lambda_1(\ddot{x}_p - \ddot{x}_{pd})] - \bar{F}_l \dot{\widehat{sgn}}(s_1) \\ &= M_p[\dddot{x}_{pd} - \lambda_1(\ddot{x}_p - \ddot{x}_{pd})] - \bar{F}_l \frac{2}{\pi}\frac{\alpha}{1 + \alpha^2 s_1^2}\dot{s}_1(F_p) \end{aligned} \tag{20}$$

Differentiating Eq. (18) then yields

$$\begin{aligned} \dot{s}_2(Q_1, Q_2) &= A_1 \dot{P}_1 - A_2 \dot{P}_2 - \dot{F}_{pd} \\ &= \frac{A_1 \beta_e}{V_1} Q_1 + \frac{A_2 \beta_e}{V_2} Q_2 - \left[\frac{A_1^2}{V_1} + \frac{A_2^2}{V_2}\right]\beta_e \dot{x}_p - \dot{F}_{pd} \end{aligned} \tag{21}$$

Recall that from Eq. (10), we should set $Q_2 = Q_{2d}$ for the sake of back pressure regulation. Therefore, the actual single control is Q_1. If we set $Q_1 = Q_{1d}$, in which the desired flow rate Q_{1d} is given by

$$Q_{1d} = \frac{V_1}{\beta_e A_1}\left\{-\frac{A_2 \beta_e}{V_2} Q_{2d} + \left[\frac{A_1^2}{V_1} + \frac{A_2^2}{V_2}\right]\beta_e \dot{x}_p + \dot{F}_{pd} - \lambda_3 s_2\right\} \tag{22}$$

where $\lambda_3 > 0$, then it is guaranteed that the second sliding manifold, $s_2(Q_1)$ converges exponentially to zero. Accordingly, we can also guarantee that $s_1 \to 0$, or $x_p \to x_{pd}$.

Finally, we can define the desired spool displacement x_{v1d} as a function of Q_{1d}

$$x_{v1d}(Q_{1d}, P_s, P_1) = \begin{cases} \frac{Q_{1d}}{C_d W}\sqrt{\frac{\rho}{2(P_s - P_1)}}, & Q_{1d} \geq 0; \\ \frac{Q_{1d}}{C_d W}\sqrt{\frac{\rho}{2(P_1 - P_t)}}, & Q_{1d} < 0. \end{cases} \tag{23}$$

Similarly, the control input is $u_1 = C(s)(x_{v1d} - x_{v1})$.

IV. Simulation

The complete simulation model is built at Matlab/Simulink (Mathworks, US). The hydraulic actuator is set according to the data sheet of the boom actuator in JCB Backhoe Loader (JCB, US). That is, the piston mass is $M_p = 34Kg$, the ram areas are $A_1 = 8 \times 10^{-3} m^2$ and $A_2 = 11.3 \times 10^{-3} m^2$, the effective length of the actuator is $1.86m$. The controller is so designed that $\lambda_1 = 100, \lambda_2 = 1000, \lambda_3 = 1000$ in Eqs. (10), (12), (22). The desired back pressure P_0 is chosen to be $2 \times 10^5 P_a$. In Fig. 4, the load force F_l should vary according to the motion of the cylinder, but remain negative to represent unidirectional load. A time-varying $F_l(t)$ is chosen to be $F_l(t) = -5000 + 200sin(10\pi t)N$. The upper bound $\bar{F}_l$ is chosen to be $8000N$ so that $\bar{F}_l > |F_l|$.

For the load sensing pump in Fig. 4, a simple model is proposed in [6]

$$P_s(s) = \frac{P_{s,ref}}{sT_p + 1} \tag{24}$$

in where T_p is the time constant of the pump. As aforementioned in section III,

$$P_{s,ref} = \begin{cases} \max(P_1, P_2) + P_m, & \dot{x}_p > 0 \\ P_2 + P_m, & \dot{x}_p \leq 0 \end{cases} \tag{25}$$

where P_m is the marginal pressure. For the sake of the pump stability, P_m should be at least $1MP_a$ [9]. In simulation, we set $P_m = 1.725MP_a$ $(250Psi)$.

The desired piston motion is set to be triangular waveform, as can be seen in Fig. 5. The multiple sliding surface controller in Section III gives a satisfactory tracking performance. In addition, the pressure signals can be seen in

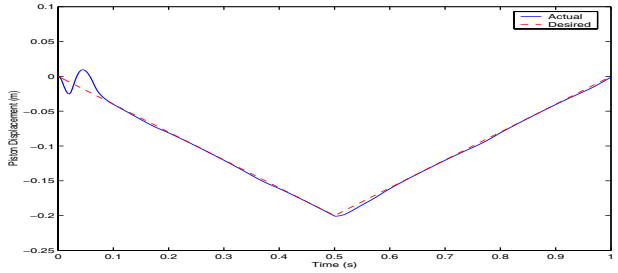

Fig. 5. Simulation results: the desired piston displacement and the actual one using the controller presented in Section III.

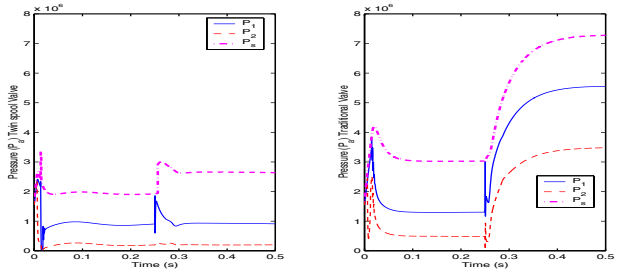

Fig. 6. Simulation results of the pressure signals. Left: the twin spool valve; right: the traditional valve.

Fig. 6. The back pressure P_2 converges to P_0 exponentially. The motion and pressure control has been accomplished successfully.

Next, we want to compare the performance of the two stage twin spool valve with that of a traditional valve. For simplicity, we choose a pilot-operated traditional valve with the exactly identical parameters to the twin spool valve. Such a two stage traditional valve can be seen in [4]. It is worth mentioning that the two displacements x_{v1} and x_{v2} are enforced to be identical. The similar trajectory tracking is achieved as well. The pressures are plotted in Fig. 6.

Now we can compare the transient power of the load sensing pump for both valves. Fig. 7 shows the transient power profile of the load sensing pump calculated by $P_s(t)Q_s(t)$, in which the supply flow rate is determined via

$$Q_s = \begin{cases} |Q_1|, & \dot{x}_p > 0 \\ |Q_2|, & \dot{x}_p \leq 0 \end{cases}$$

From Fig. 7, we notice the tremendous energy saving for the twin spool valve compared to the traditional valve.

V. Energy-saving discussion

In this section, we will address the issue that how the energy can be saved as the load sensing pump is utilized. For simplicity, we just conduct the quasi-steady analysis on the energy efficiency, in which we assume the supply flow rate Q_s is constant. Without loss of generality, define the area ratio of the cylinder in Fig. 4 as $\gamma := A_1/A_2 < 1$. In the following section, we will formulate the pressure signals P_s, P_1, P_2 with respect to the marginal pressure P_m and the external load F_l.

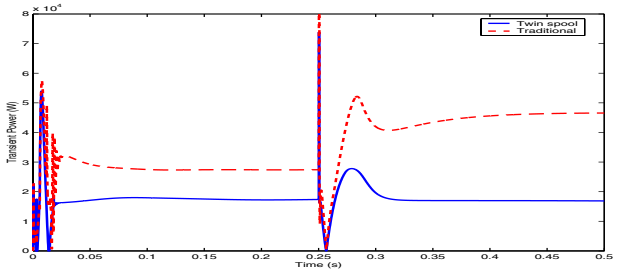

Fig. 7. Simulation results of the transient power of the load sensing pump for the traditional valve (dashed line) and the twin spool valve (solid line).

A. Traditional valve

1) $\dot{x}_p > 0$: Eqs. (8) (9) and $x_{v1} = x_{v2} > 0$ can be combined to give the following relation:

$$P_s = P_1 + \gamma^2 P_2 \tag{26}$$

From Eq. (7), as well as $\ddot{x}_p = 0$ due to the quasi-steady assumption, we have

$$P_1 A_1 - P_2 A_2 + F_l = 0 \tag{27}$$

Eqs. (24) (25) give

$$P_s = P_1 + P_m \tag{28}$$

since $P_1 > P_2$.

Then from Eqs. (26) (27) (28), we have the pressures of the traditional valve $P_{s,R}, P_{1,R}, P_{2,R}$ with respect to P_m and F_l:

$$\begin{aligned} P_{s,R} &= \frac{1+\gamma^3}{\gamma^3} P_m + \frac{1}{\gamma}\frac{-F_l}{A_2} \\ P_{2,R} &= \frac{1}{\gamma^2} P_m \\ P_{1,R} &= \frac{1}{\gamma^3} P_m + \frac{1}{\gamma}\frac{-F_l}{A_2} \end{aligned} \tag{29}$$

2) $\dot{x}_p \leq 0$: Likewise, Eqs. (8) (9) and $x_{v1} = x_{v2} < 0$ can be combined to give the following relation:

$$P_s = \frac{1}{\gamma^2} P_1 + P_2 \tag{30}$$

Then Eqs. (30) (27) (28) give

$$\begin{aligned} P_{s,R} &= \frac{\gamma^3+1}{\gamma^3+1-\gamma^2} P_m + \frac{\gamma^2}{\gamma^3+1-\gamma^2}\frac{-F_l}{A_2} \\ P_{2,R} &= \frac{\gamma^3}{\gamma^3+1-\gamma^2} P_m + \frac{\gamma^2-1}{\gamma^3+1-\gamma^2}\frac{-F_l}{A_2} \\ P_{1,R} &= \frac{\gamma^2}{\gamma^3+1-\gamma^2} P_m + \frac{\gamma^2}{\gamma^3+1-\gamma^2}\frac{-F_l}{A_2} \end{aligned} \tag{31}$$

B. Twin spool valve

We denote its corresponding pressures to be $P_{s,W}, P_{1,W}, P_{2,W}$.

1) $\dot{x}_p > 0$: Note that the back pressure regulation $P_{2,W} = P_0$. From Eqs. (27) (28), the pressures can be expressed as a function of P_0, P_m, F_l:

$$\begin{aligned} P_{s,W} &= \frac{1}{\gamma}P_0 + \frac{1}{\gamma}\frac{-F_l}{A_2} + P_m \\ P_{2,W} &= P_0 \\ P_{1,W} &= \frac{1}{\gamma}P_0 + \frac{1}{\gamma}\frac{-F_l}{A_2} \end{aligned} \tag{32}$$

2) $\dot{x}_p \leq 0$: It is easy to get that regardless of the piston moving direction ($\dot{x}_p$), $P_{1,W}, P_{2,W}$ are identical to Eq. (32). However, Eq. (25) yields a different supply pressure

$$P_{s,W} = P_0 + P_m \tag{33}$$

C. Energy saving

For the traditional valve, the required pump work is $P_R Q_s$; while for the twin spool valve, the pump needs to provides $P_W Q_s$. From Eqs. (29) (31) (32) (33), the power the twin spool valve saves $\Delta W := (P_R - P_W)Q_s$, is given by

$$\Delta W = \begin{cases} (\frac{1}{\gamma^3}P_m - \frac{1}{\gamma}P_0)Q_s, & \dot{x}_p > 0 \\ (\frac{\gamma^2}{\gamma^3+1-\gamma^2}P_m + \frac{\gamma^2}{\gamma^3+1-\gamma^2}\frac{-F_l}{A_2} - P_0)Q_s, & \dot{x}_p \leq 0 \end{cases} \tag{34}$$

Clearly, ΔW is positive if $P_m > P_0$ and $F_l < 0$.

In general, the energy supplied by the pump mainly interacts with the external mechanical power. Meanwhile, the energy is dissipated in meter-in and meter-out orifices. In Fig. 8, the diagram of the energy distribution is plotted for both $\dot{x}_p \leq 0$ and $\dot{x}_p > 0$. Area (1) represents the energy loss in the meter-in orifice. Area (4) represents the energy loss in the meter-out orifice. For instance for $\dot{x}_p \leq 0$, the flow meters out of the P_1 chamber into the tank. The power loss is $P_1 Q_1$, or $P_1 \gamma Q_s$. For $\dot{x}_p > 0$, the power loss in the meter-out orifice is $P_2 Q_2$, or $P_2 \frac{1}{\gamma} Q_s$. Area (3), identical to area (4), is a function of Q_s for the sake of comparison.

Recall the unidirectional load $F_l < 0$. For $\dot{x}_p \leq 0$, $F_l \dot{x}_p \geq 0$. In other words, the external load injects energy (2) into the hydraulic systems. Those energy, as well as those from the pump, are consumed in the orifices. We have $P_s Q_s + (2) - (1) - (3) = 0$. For $\dot{x}_p > 0$, the pump provides both the useful work outwardly and the wasted energy in the orifices. We have $P_s Q_s - (1) - (2) - (3) = 0$.

Since the identical marginal pressures P_m are used, the wasted works due to meter-in orifice (1) are identical. Therefore, the energy-saving feature showed in Eq. (34) is contributed by the reduction of the loss in the meter-out orifice via back pressure regulation.

Using the quasi-steady method and the parameters in Section IV, we can estimate the power consumption for the traditional valve and the twin spool valve. The ratio of the power $P_{s,W}/P_{s,R}$ is approximately 66.3% and 36.3%, for $\dot{x}_p \leq 0$ and $\dot{x}_p > 0$ respectively. The estimates have a perfect agreement with the dynamic simulation results in Section IV (see Fig. 7, $t \in [0, 0.25]s$ corresponds to the case where $\dot{x}_p \leq 0$, and $t \in [0.25, 0.5]s$ corresponds to that where $\dot{x}_p > 0$).

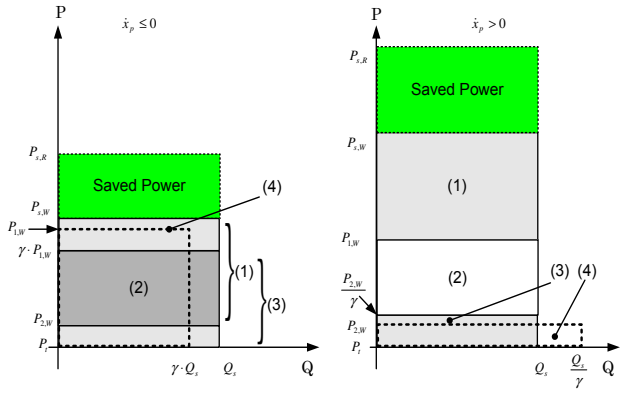

Fig. 8. Quasi-steady analysis of energy consumption of the load sensing pump for $\dot{x}_p \leq 0$ (left) and $\dot{x}_p > 0$ (right). Area (1) represents the energy loss in the meter-in orifice; Area (2) is associated with the work of the external load; Area (4) (enclosed by dashed-line) stands for the energy loss in the meter-out orifice; For the sake of comparison, area (4) is represented to be area (3).

VI. Conclusion

In this paper, a control scheme is developed for a two stage twin spool valve with energy-saving feature in mobile hydraulics. It is found that it can save the extra energy even with load-sensing pumps. A scenario with a load-sensing pump where the valve is used to control the double-acting hydraulic actuator in the presence of large unidirectional (gravitational) load forces, is taken into account. The multiple surface sliding mode controller is designed to regulate the pressure and achieve the motion control. The simulation study verifies that significant energy-saving has been achieved by regulating the back pressure.

References

[1] T. J. Kappi, "Modeling and simulation utilized in research and development of mobile hydraulics," in *Proceedings of 1st FPNI-PhD Symposium*, Hamburg, Germany, 2000, pp. 353–61.

[2] R. Manasek, "Simulation of a electrohydraulic load-sensing system with ac motor and frequency changer," in *Proceedings of 1st FPNI-PhD Symposium*, Hamburg, Germany, 2000, pp. 311–24.

[3] R. T. Anderson and P. Y. Li, "Mathematical modeling of a two spool flow control servovalve using a pressure control pilot," *Transactions of ASME. Journal of Dynamic Systems, Measurement and Control*, vol. 124, pp. 420–427, Sep 2002.

[4] P. Y. Li, "Dynamic redesign of a flow control servovalve using a pressure control pilot," *Transactions of ASME. Journal of Dynamic Systems, Measurement and Control*, vol. 124, pp. 428–434, Sep 2002.

[5] H. E. Merritt, *Hydraulic Control System*. John Wiley and Sons, 1967.

[6] M. Jelali and A. Kroll, *Hydraulic Servo-systems: Modeling, Identification and Control*. Springer, 2003.

[7] M. Won and J. K. Hedrick, "Multiple-surface sliding control of a class of uncertain nonlinear systems," *International Journal of Control*, vol. 64, pp. 693–706, 1996.

[8] H. K. Khalil, *Nonlinear System, Third Edition*. Prentice Hall, 2002.

[9] D. Wu, "Modeling and experimental evaluation of a load-sensing and pressure compensated hydraulic system," PhD Thesis, University of Saskatchewan, Saskatchewan, Canada, Dec 2003.